Site-directed mutagenesis of the type II TGF-β receptor indicates a ligand-binding site distinct from that of the type II activin receptor

Alain Guimond[1], Traian Sulea[1], Ally Pen, Pohien Ear, Maureen D. O'Connor-McCourt*

Biotechnology Research Institute, National Research Council of Canada, 6100 Royalmount Avenue, Montréal, QC H4P 2R2, Canada

Received 21 January 2002; accepted 22 January 2002

First published online 22 February 2002

Edited by Veli-Pekka Lehto

Abstract Site-directed mutagenesis was used to map the ligand-binding surface of the type II transforming growth factor-β receptor extracellular domain (TβRII-ECD). Two putative ligand-binding sites were probed, the first being a predicted hydrophobic patch, the second being the finger 1 surface loop. Nine residues were mutated in the context of full-length TβRII and the effect of these mutations on ligand-binding and receptor signaling was analyzed. Complementary information was obtained by examining 'natural' evolutionary TβRII mutations. Together, the results indicate that residues within the finger 1 region, but not the hydrophobic patch, of the TβRII-ECD are required for productive ligand-binding. We conclude that, surprisingly, the ECDs of TβRII and type II activin receptor utilize distinct interacting surfaces for binding their respective ligands.

Key words: Type II transforming growth factor-β receptor ectodomain; Mutagenesis; Ligand-binding; Signaling; Structure–function analysis; Type II activin receptor

1. Introduction

Transforming growth factor-β (TGF-β) is a member of a family of dimeric polypeptides that includes bone morphogenetic proteins and activins [1,2]. The signaling pathways that are stimulated by TGF-β regulate many critical cellular processes such as cell growth, differentiation, extracellular matrix deposition and immune function [1,2]. Most biological effects of TGF-β are mediated by the type I (TβRI) and type II (TβRII) cell surface receptors, which are both required for TGF-β signaling [3,4]. Previous studies on TGF-β signaling [5,6,7–10] have suggested that TβRII, a constitutively activated kinase, is the primary sensor for the presence of TGF-β and that, after the initial ligand-binding event, the TGF-β/TβRII complex recruits and phosphorylates TβRI, which then propagates a signal to downstream substrates. Dissecting the structural basis for the high affinity interaction between TGF-β and TβRII is of fundamental importance towards understanding the initial molecular events in the activation of TGF-β signaling pathways. It will also provide useful molecular design strategies towards modulating the many important effects of TGF-β.

In two previous studies, using a scanning-deletion mutagenesis approach combined with a homology model of the TβRII extracellular domain (TβRII-ECD), we delineated the core ligand-binding domain of TβRII and identified two regions within this core domain as putative ligand-binding sites [11,12]. The first region is an extended hydrophobic patch on the concave face of the ECD while the second site is the finger 1 surface loop of the ECD. Mutational analysis of a hydrophobic patch on the mouse type II activin receptor (ActRII)-ECD that is similar to the one on the TβRII-ECD demonstrated that it forms a critical ligand-binding surface for activin and inhibin, supporting the idea that this region may form a ligand-binding site on the TβRII-ECD [13]. To verify the function of the hydrophobic patch and finger 1 regions on the TβRII-ECD, we have now analyzed the effect of introducing single-residue mutations into these sites on ligand-binding as well as receptor signaling. As a complement to this site-directed mutational approach, we also examined the 'natural' mutagenesis of TβRII that occurred during evolution by aligning TβRII-ECD sequences from various species. Taken together, our results demonstrate that residues within the finger 1 region, but not the hydrophobic patch, of the TβRII-ECD are important for productive ligand-binding, thereby demonstrating that the ECDs of TβRII and ActRII utilize distinct interacting surfaces for binding their respective ligands.

2. Materials and methods

2.1. Mutagenesis

Mutagenesis of the human TβRII coding region subcloned in pCDNA-3 (Invitrogen) was done by site-directed mutagenesis [14]. Primers used in this analysis are as follows: 5′ and 3′ common primers are, respectively, II-1: 5′-AAGCTTCACCATGGAGGCGGCG, and AS.1: 5′-TTGTGGTTGATGTTGTTGG. Mutagenic primers are as follows, with only the forward primer shown, the reverse primer being its exact complement (names correspond to the position of the mutated amino acid on the human cDNA):

C67A.gen: 5′-GCAGTTGCTCATGGCGGATTTCTGGTTG, C71A.gen: 5′-GCATGAGCAACGCCAGCATCACC, V85A.gen: 5′-GGAAGTCTGTGCGGCTGTATGG, V87A.gen: 5′-GTCTGTGTGGCTGCATGGAGAAAG, L97A.gen: 5′-CGAGAACATAACAGCAGAGACAGTTTG, E98A.gen: 5′-AGAACATAACACTAGCGACAGTTTGCC, E98Q.gen: 5′-AGAACATAACACTACAGACAGTTTGCC, V100A.gen: 5′-AACACTAGAGACAGCTTGCCATGACC, F133A.gen: 5′-CCTGGTGAGACTGCCTTCATGTGTTCC, M135A.gen: 5′-GGTGAGACTTTCTTCGCGTGTTCCTGTAGC.

*Corresponding author. Fax: (1)-514-496-5143.
E-mail address: maureen.o'connor@nrc.ca (M.D. O'Connor-McCourt).

[1] These authors contributed equally to this work.

Abbreviations: TGF-β, transforming growth factor-β; TβRII, type II TGF-β receptor; ActRII, type II activin receptor; ECD, ectodomain

0014-5793/02/$22.00
PII: S0014-5793(02)02378-5

2.2. Cell culture and transfection

HEK 293 cells were maintained in Dulbecco's modified Eagle's media (DMEM; Gibco) supplemented with 10% fetal bovine serum (FBS; Gibco). All transfections were done in six- or 12-well plates using the SuperFect reagent (Qiagen) according to the manufacturer's protocol unless otherwise specified.

2.3. Surface expression

HEK 293 cells were seeded in six-well dishes and transfected using 2 μg of DNA and 5 μl of SuperFect reagent according to the manufacturer's protocol. 48 h after transfection the cells were re-suspended in cold DMEM–10% FBS for 30 min at 4°C. Cells were then incubated for 1 h at 4°C in the presence of an anti-TβRII antibody (R&D Systems) directed against the ECD. After washing in cold DMEM–10% FBS, the cells were incubated for 1 h with an FITC conjugate goat anti-rabbit IgG (Sigma) diluted 1/100. Cells were then washed in cold DMEM–10% FBS and analyzed by flow cytometry on an EPICS® XL-MCS (Beckman-Coulter®).

2.4. Cross-linking ligand-binding assay

48 h after transfection, the cells were incubated with 100 pM of [I^{125}]TGF-β1 for 2–3 h. After washing with D-PBS^{++}, the receptor-bound ligand was cross-linked with BS^3 (Pierce) for 5 min followed by an additional 5 min in 100 mM glycine to stop the reaction. Total protein was then extracted in solubilization buffer (1% Triton X-100, 10% glycerol, 20 mM Tris–HCl pH 7.4, 1 mM EDTA and PMSF) at 4°C for 30 min.

2.5. Direct ligand-binding assay

HEK 293 cells were transfected in triplicate as previously described. 48 h after transfection the cells were incubated for 2 h on ice with 100 pM [I^{125}]TGF-β1 with or without 10 nM of unlabeled TGF-β1 as specific competitor in the binding buffer (D-PBS^{++}, 0.1% BSA). Cells were washed for 2–3 min with 500 μl of binding buffer, then acid-washed (150 mM NaCl, 0.1% acetic acid) twice for 2 min to recover bound ligand. The two acid washes were pooled and counted on a gamma counter. For each mutant tested, the counts obtained from the competed samples were subtracted from the total counts (non-competed) to determine specific binding. In the case of the fast washing procedure, cells were washed for less than 5 s with 500 μl of binding buffer.

2.6. Smad2 phosphorylation signaling assay

HEK 293 cells were transiently cotransfected in triplicate with Flag-Smad2 (generously provided by Dr. L. Attisano, University of Toronto, Toronto, Canada) and the indicated TβRII mutant plasmids in a 1:1 ratio using the SuperFect reagent. Total DNA was kept constant by adding pCDNA-3. 24 h after transfection, the cells were incubated in DMEM without serum (DMEM-0) for 2–4 h, and then incubated with or without 400 pM of TGF-β1 for 15–20 h. Cells were then washed twice with PBS and the protein was extracted in solubilization buffer at 4°C for 30 min. The amount of protein was quantified using BCA reagent (Pierce) and 3 μg of protein from each sample was loaded onto 10% SDS–polyacrylamide gels. The protein was transferred onto Immobilon-P membranes (Millipore), which were rinsed in water for 2 min, then in methanol for 2 min, and air-dried. The dry membranes were then incubated with the appropriate primary antibody diluted in 5% skim milk/TBS overnight at 4°C. The membranes were then washed 4×15 min with TBS-Tween 0.05% and incubated with horseradish peroxidase-conjugated anti-rabbit or anti-mouse IgG secondary antibody (Jackson) at 1/10 000 dilution in 5% skim milk/TBS at room temperature for 1 h. After extensive washing, the signals were revealed with ECL detection reagents (Renaissance-ECL kit, NEN). The anti-phospho-Smad2 primary antibody (Geneka Biotechnology) was used at a 1/1000 dilution, the M2 anti-Flag antibody (Kodak) was used at a 1/5000 dilution and the anti-hTβRII-ECD antibody (2379; produced in our laboratory) was used at a 1/1000 dilution. The same membranes were stripped and re-probed to monitor expression levels of the transfected plasmids.

2.7. Statistics

Data were analyzed by one-way analysis of variance using $P > 0.05$ as significance criterion. Post-hoc analysis relied on Dunnett's multiple comparison test using the Prism software (GraphPad Software Inc.).

3. Results

3.1. Design of TβRII mutants

We have previously delineated the core ligand-binding domain of the full-length human TβRII using a scanning-deletion mutagenesis approach [11]. We then extended the scanning-deletion mutagenesis analysis to within the core ligand-binding domain itself, and rationalized the results using a homology model of the TβRII-ECD structure that was based on the crystal structure of the ECD of the mouse ActRII [12].

In that study, a solvent-exposed hydrophobic patch lining the concave face of the TβRII-ECD modeled structure was identified as a potential protein-binding interface and was suggested to be a putative ligand-binding site [12]. A similar hydrophobic patch exists on the ActRII-ECD structure [15]. Mutational analysis of mouse ActRII demonstrated that three residues, F42, W60, and F83 from this hydrophobic site, form a critical binding surface required for functional interactions with both activin and inhibin [13]. In this report, in order to verify whether the corresponding hydrophobic site on TβRII-ECD is implicated in binding the TGF-β ligand, we individually mutated six hydrophobic residues, V85, V87, L97, V100, F133, and M135, to alanine in the context of the full-length human TβRII. Residues V85 and M135 of human TβRII correspond to ligand-binding site residues F42 and F83 of mouse ActRII, respectively. In addition, the role of a negatively charged residue, E98, which is adjacent to this hydrophobic patch, was explored by generating two mutants, E98Q and E98A. The search for a negatively charged residue on TβRII that may be involved in ligand-binding was motivated by the finding that a positively charged residue, R94, of the TGF-β1 ligand is important for binding to TβRII [16]. Since the side chains of all these mutated residues are predicted to be exposed at the protein surface, the risk of introducing significant conformational changes upon mutation is low.

Out of the five structurally variable regions identified between the TβRII-ECD model and ActRII-ECD structure, three represent insertions in TβRII-ECD relative to ActRII-ECD. Our previous scanning-deletion mutagenesis results indicated that two of these larger surface loops in TβRII-ECD can be partially deleted without affecting TGF-β-binding, and that only one of them, the so-called finger 1, might form a

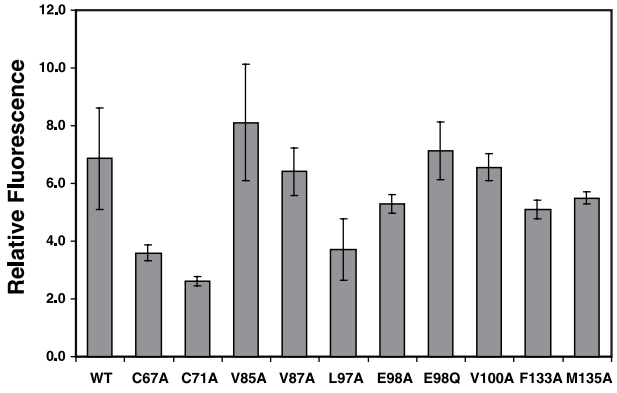

Fig. 1. Surface expression of TβRII mutants. Transiently transfected HEK 293 cells were incubated with an antibody directed against the TβRII-ECD and detected by flow cytometry analysis with an FITC-conjugated secondary antibody (see Section 2). Histograms show the mean fluorescence values calculated from at least three independent experiments.

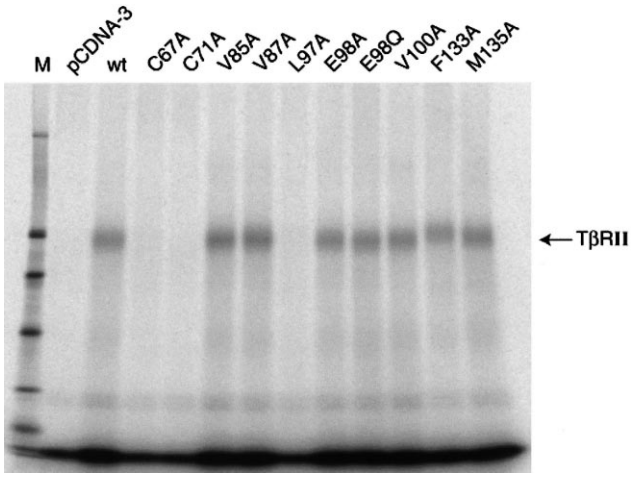

Fig. 2. Ligand cross-linking to TβRII mutants. HEK 293 cells were transiently transfected with wild-type or mutant TβRIIs followed by cross-linking to [I^{125}]TGF-β1. Labeled receptors were resolved on 4–12% gradient gels and exposed to phosphorimager screens. Mutants are labeled in the respective lanes. M: molecular weight marker. The arrow indicates the TβRII band.

binding interface with the ligand [12]. Finger 1 appears as a unique, distinctive structural feature of TβRII in that it contains four additional cysteine residues outside the canonical pattern of cysteine residues characteristic of the 'three-finger toxin' fold. Knowledge-based modeling predicted that the finger 1 of TβRII-ECD would contain two disulfide bonds, C54–C71 and C61–C67 [12]. Two mutants were thus generated, C67A and C71A, in order to investigate the role of these disulfide bonds in constraining a putative bioactive conformation adopted by the finger 1 of TβRII. Because of the significant sequence variability of the finger 1 in the 'three-finger toxin' fold family [15], these mutations are expected not to disrupt the fold of the ECD structure.

3.2. Surface expression of TβRII mutants

We examined the level of expression of the 10 TβRII point mutants at the surface of transiently transfected HEK 293 cells by flow cytometry analysis using an ECD-directed antibody (Fig. 1). HEK 293 cells were chosen because they express very low levels of endogenous TGF-β receptors and because they are transfected with high efficiency. Seven of the receptor mutants were expressed at levels comparable with that of the wild-type receptor. The remaining three mutants, C67A, C71A, and L97A, displayed approximately half of the wild-type TβRII expression level. These results indicate that the TβRII mutants are expressed and transported to the cell surface, which suggests that no major conformational alteration of the ECD structure as a whole (i.e. unfolding or misfolding) was introduced upon mutation.

3.3. Ligand-binding by TβRII mutants

We evaluated the ligand-binding properties of the TβRII mutants in HEK 293 cells by covalently cross-linking the radiolabeled TGF-β1 ligand to the mutant receptors. We also verified ligand-binding in a direct binding assay using radiolabeled and unlabeled TGF-β1 (see Section 2). As shown in Fig. 2, similar levels of cross-linked ligand–receptor complexes were detected for the wild-type receptor and seven TβRII mutants targeting residues on the concave face of the ECD: V85A, V87A, E98A, E98Q, V100A, F133A, and M135A. No cross-linked receptors were detected when the vector alone was transfected, confirming the low level of endogenous TβRII. These results indicate that the TGF-β-binding site does not correspond to the hydrophobic patch on the concave side of TβRII-ECD, and that the acidic residue E98 is not engaged in specific electrostatic interactions with the ligand. Importantly, since mutation of residues V85 and M135, which correspond to the activin- and inhibin-binding site residues F42 and F83 of ActRII-ECD, did not affect TGF-β-binding, our data indicate that TβRII and ActRII utilize distinct, non-overlapping surfaces for binding their respective ligands.

Three TβRII mutants could not be cross-linked to [I^{125}]TGF-β1 (Fig. 2). They correspond to the alanine mutation of two cysteine residues, C67 and C71 from finger 1, and of a hydrophobic residue, L97, from the concave face of the ECD. These three mutants are expressed at the cell surface at approximately half the level of the wild-type TβRII (Fig. 1), which is well within the detection range of the cross-linking assay. Therefore, although these three TβRII mutants are present at the surface of the HEK 293 cells, they cannot be efficiently cross-linked to the ligand, presumably due to impaired ligand–receptor interactions upon mutation.

To verify this lack of ligand-binding, we employed a different assay that does not involve covalent ligand–receptor cross-linking. Since cross-linking reactions are highly dependent on the proximity of the reacting groups, ligand-binding might not

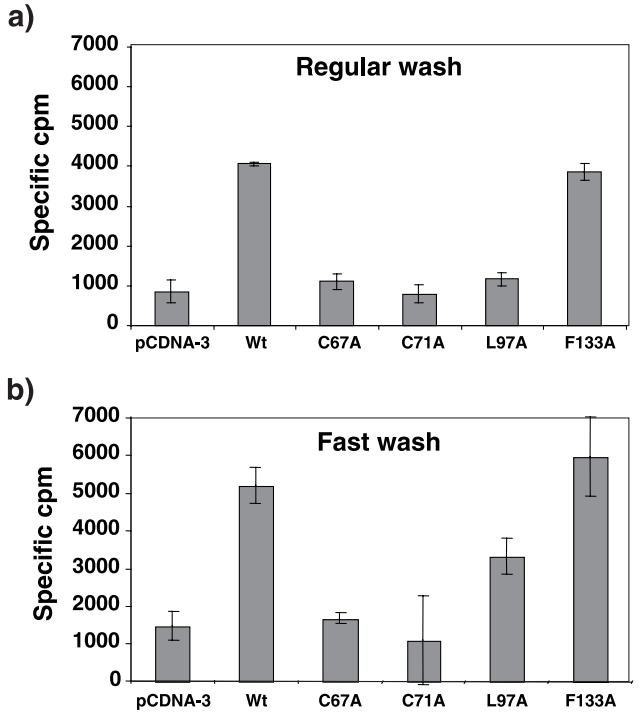

Fig. 3. Direct ligand-binding to TβRII mutants. Transiently transfected HEK 293 cells were incubated with [I^{125}]TGF-β1 in the presence (competed) or absence of 100-fold excess of unlabeled TGF-β1. Surface-bound ligand was recovered by two acidic washing steps after removal of the excess ligand by (a) a regular washing protocol or (b) a fast washing protocol (see Section 2). Histograms show the mean value calculated from three independent experiments. Data are expressed as specific counts obtained for the wild-type TβRII, and were calculated by subtracting counts from competed samples from counts from non-competed sample.

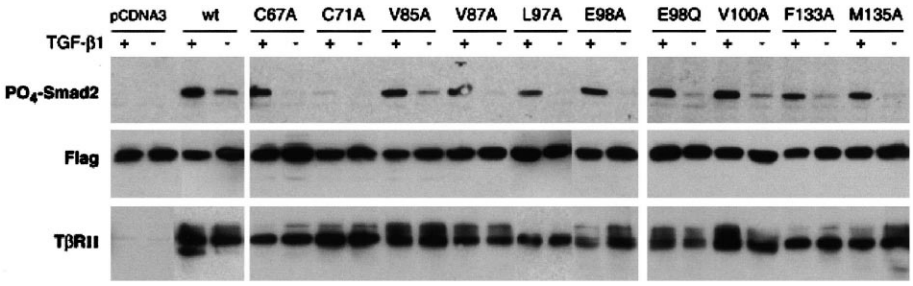

Fig. 4. Smad2 phosphorylation signaling by TβRII mutants. Wild-type or mutant TβRII was cotransfected with Flag-tagged Smad2 and the cells treated (+) or not (−) with TGF-β1. Phosphorylated Smad2 was revealed by Western blot with and anti-phospho-Smad2 antibody (PO_4-Smad2). Expression level of Flag-Smad2 was detected with and anti-Flag antibody and is shown on the middle panel (Flag). Expression of transfected receptors was detected with an anti-TβRII-ECD antibody (TβRII) and is shown on the bottom panel.

be detected due to subtle changes in the positioning of the reacting groups that could occur upon mutation. Wild-type and selected TβRII mutants (C67A, C71A, L97A, and F133A) were transfected in HEK 293 cells and incubated in the presence of [I^{125}]TGF-β1 with or without a 100-fold excess of unlabeled TGF-β1 competitor. After washing off unbound ligand, receptor-bound ligand was recovered. The counts from samples with competitor were subtracted from the counts from samples without competitor to obtain specific binding. As expected (see Fig. 3a) the level of specific binding obtained with mutant F133A was similar to the level obtained with the wild-type receptor. On the other hand, the level of specific

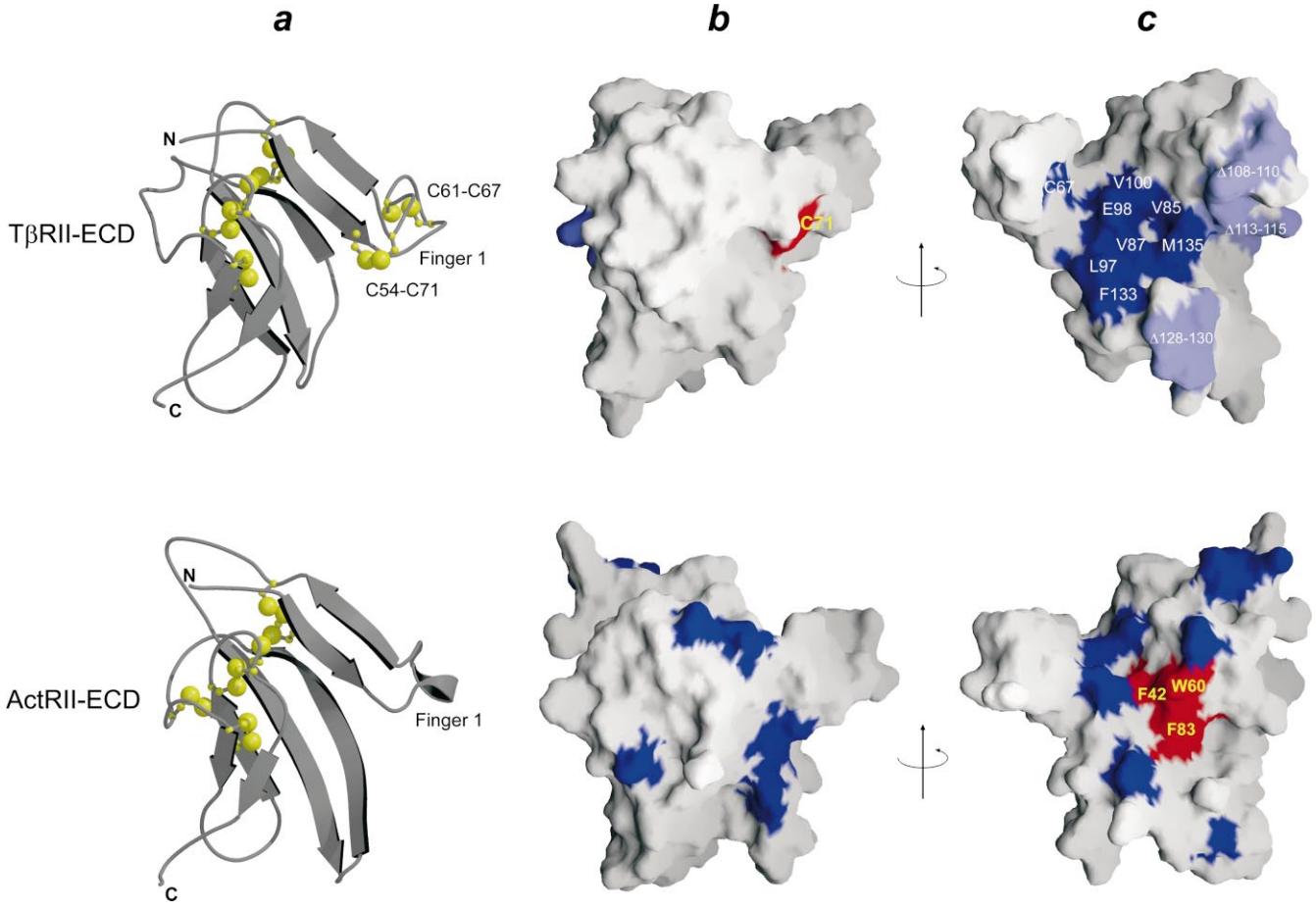

Fig. 5. Mapping of the mutagenesis data onto the modeled structure of TβRII-ECD [12] (upper panels) and crystal structure of ActRII-ECD [15] (lower panels). a: Ribbon diagrams of the ECD structures, with cysteine side chains displayed as ball and stick representation with yellow atoms. The orientation of the two ECDs corresponds to their structural alignment. b: Molecular surface representation of the ECD structures displayed with the convex side in front in an orientation similar to that shown in (a), and (c) with the concave side in front corresponding to ~180° rotation relative to the orientation in (a) and (b). The molecular surface patches associated with the side chains of TβRII residues mutated to alanine in this study and of ActRII residues mutated to alanine in [13] are color-coded. Red surface areas correspond to side chains identified as being required for a functional interaction with the respective ligands of each receptor, and blue coloring corresponds to side chains not required for functional ligand-binding. Surface areas corresponding to individual three-residue deletions within the core ligand-binding domain of TβRII that were shown not to alter ligand-binding [12] are colored in light blue.

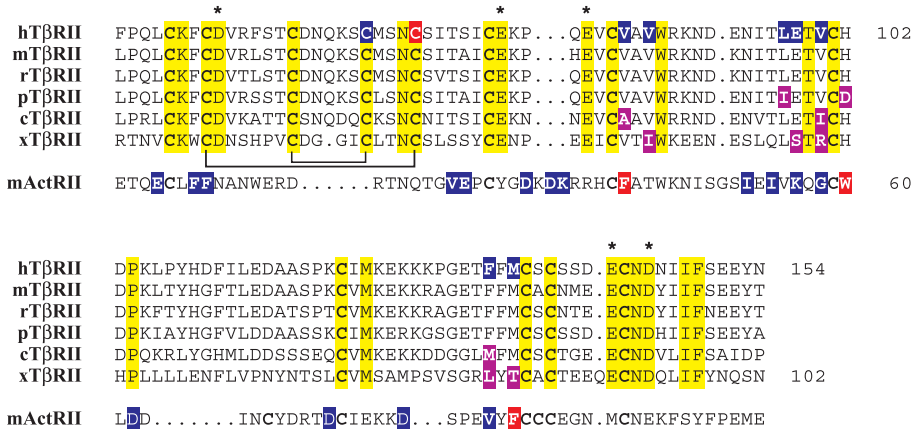

Fig. 6. Sequence alignment of the ECDs from TβRII species homologues. h – human, m – mouse, r – rat, p – pig, c – chicken, x – *X. laevis*. The sequence of mouse ActRII ECD is also aligned. Cysteine residues are shown in bold. Predicted disulfides in the finger 1 of TβRII-ECD are indicated. Identical residues across the TβRII-ECD alignment are highlighted on a yellow background. TβRII residues identified in this study as being required for functional binding to TGF-β, and ActRII residues identified in [13] as being critical for functional binding to activin are shown on a red background. The other residues investigated by mutagenesis, and which have no effect on the functional binding of the respective ligands, are shown on a blue background. 'Natural mutations' within the TβRII species homologues that correspond to positions mutated in this study are highlighted on a violet background. Asterisks indicate identical acidic residues across the TβRII-ECD alignment.

binding for mutants C67A, C71A, and L97A did not differ significantly from the pCDNA-3 control, indicating that the interaction between TGF-β1 and these receptor mutants could not be detected. If the ligand has a lower affinity for these mutants due to a faster dissociation rate, bound ligand might dissociate from the receptor during the washing step and no interaction would be detected. To further clarify this issue, we repeated the experiment with a very fast washing step before the recovery of the bound ligand (see Section 2). When using this approach, specific ligand-binding to mutant F133A remained similar to that of the wild-type receptor, while specific binding to both C67A and C71A mutants was still not significantly different from the pCDNA-3 control (Fig. 3b). These results remain consistent with those from the covalent ligand–receptor cross-linking assay (Fig. 2). However, we observed a significant amount of bound ligand for the L97A mutant (~230% relative to the pCDNA-3 control and ~65% relative to the wild-type receptor), indicating that TGF-β1 binds to the L97A receptor mutant, but that it likely dissociates from it at a fast rate.

3.4. TGF-β signaling by TβRII mutants

It is currently accepted that binding of TGF-β to TβRII leads to recruitment and phosphorylation of TβRI [5,6], which then triggers several signaling pathways by activating downstream targets such as the Smad family of proteins [17–19]. It is therefore conceivable that any significant decrease in ligand–TβRII binding affinity (e.g. attainable here by point mutations of the receptor) would impair the TGF-β signaling function. We tested the ability of TβRII mutants to mediate a functional TGF-β response in intact cells by using a Smad2 phosphorylation assay. The TβRII mutants were transiently cotransfected with Flag-Smad2 in HEK 293 cells. As demonstrated by the receptor–ligand cross-linking experiments (Fig. 2), these cells express very low levels of endogenous TGF-β receptors; however, the amount of endogenous TβRI is sufficient to support ligand-dependent phosphorylation of transfected Smad2 in the presence of cotransfected TβRII. The level of expression of the TβRII mutants and the level of Smad2 phosphorylation achieved by those mutants were monitored by Western blot analysis. As shown in Fig. 4, ligand-stimulated Smad2 phosphorylation was detected for nine out of the 10 TβRII mutants investigated, indicating that these are functional receptor mutants that are able to participate in signaling competent heteromeric receptor complexes in the presence of the TGF-β ligand. C71A was the only inactive mutant in the Smad2 phosphorylation assay. Except for the C67A mutant which displayed ligand-dependent signaling, but lacked detectable ligand-binding, the results obtained from the signaling assay were in agreement with the ligand-binding data (Figs. 2 and 3). Our combined results indicate that the side chains of seven residues within the hydrophobic patch on the concave side of the TβRII-ECD are not important for ligand-binding, and are not required for ligand-dependent signaling towards the intracellular downstream target, Smad2. Residue C71 in the finger 1 of the ECD is required for both ligand-binding and signaling. The disagreement between the signaling and ligand-binding assays for the C67A mutant may result from this mutant-binding ligand with a very fast dissociation rate, such that radioligand-binding and cross-linking were undetectable, while receptor signaling was ligand-dependent.

4. Discussion

In order to map the TGF-β-binding site of TβRII, we generated a set of single-residue mutations within the ECD of the full-length human receptor. The design of these mutants was based on previous data that we obtained by combining scanning-deletion mutagenesis of TβRII with a homology model of the TβRII-ECD structure [12]. In that report, two regions on TβRII-ECD were identified as putative binding sites (see also Section 3.1). The first one is an extended hydrophobic patch on the concave face of the ECD. The second region is the finger 1 surface loop of the ECD. To investigate these two regions further, we introduced 10 single-residue mutations targeting nine residues into full-length TβRII (Fig. 5). The resulting mutants were tested for their ability to bind the TGF-β1 ligand as well as to support a functional TGF-β response in intact cells.

Seven mutations that were introduced on the hydrophobic surface on the concave side of the ECD, V85A, V87A, E98A, E98Q, V100A, F133A, and M135A, did not affect ligand-binding, as shown independently by covalent ligand–receptor cross-linking and direct binding assays (Figs. 2 and 3). Although ligand–receptor cross-linking was not detected for the L97A mutant, a fast washing procedure applied in the direct binding assay revealed significant ligand-binding to this mutant (Fig. 3b). Furthermore, all of these eight receptor mutants were able to support a ligand-dependent functional response as demonstrated in a Smad2 phosphorylation signaling assay (Fig. 4). Taken together, these data demonstrate that the hydrophobic patch on the concave side of the ECD does not form a critical binding surface required for functional interactions with TGF-β. This is also consistent with our previous results showing that three-residue deletions introduced in two surface loops that are adjacent to this region do not alter ligand-binding significantly (Fig. 5c). In addition, the data obtained for the mutants E98A and E98Q demonstrate that residue E98, which is located near this hydrophobic patch, does not represent the direct binding partner for the critical residue R94 of the TGF-β1 ligand [16].

Structural studies have shown the existence of a similar hydrophobic surface on the concave side of the ECD of ActRII [15]. A mutational analysis of the full-length mouse ActRII, in which 19 solvent-exposed residues of the ECD were individually mutated to alanine, has recently been published [13]. In that study, three residues, F42, W60, and F83, that cluster on the hydrophobic surface on the concave side of ActRII-ECD (Fig. 5), were identified as being required for both activin- and inhibin-binding and for a functional activin response in intact cells. Residues F42 and F83 correspond to the human TβRII residues V85 and M135 that we mutated in this study to alanine, with no significant effect on ligand-binding and signaling properties of the receptor. Hence, it appears that despite the predicted similarities in fold topology, the ECDs of TβRII and ActRII utilize distinct interacting surfaces for binding their respective ligands (Fig. 5).

A striking difference between TβRII-ECD and ActRII-ECD is a surface loop called finger 1, which contains an insertion of six residues as well as four additional cysteine residues relative to ActRII. Homology modeling of the TβRII-ECD structure predicted formation of two disulfide bonds in finger 1 [12], C54–C71 at the loop-anchor positions, and C61–C67 in the middle of the loop (Fig. 5a). In addition to these unique structural features, we previously found that three-residue deletions in finger 1 abolish ligand-binding [12]. We hypothesized that finger 1 could be implicated in functional interactions with TGF-β, which prompted us to generate in this study two TβRII mutants, C67A and C71A, each predicted to have a disruption of one of the two disulfide bonds in finger 1 of the ECD. The mutation of residue C71 to alanine abolished both the ligand-binding and signaling capabilities of TβRII. In contrast, mutant C67A exhibited a positive functional response to TGF-β in the Smad2 phosphorylation assay, although we were unable to detect ligand-binding to this mutant. Thus, it appears that the disruption of the predicted disulfide bond C54–C71 at the anchor of finger 1 has a more pronounced effect than disruption of the predicted disulfide bond C61–C67 within the finger 1 itself. In the modeled structure of TβRII-ECD, the disulfide C54–C71 is solvent-exposed (Fig. 5b), and could directly interact with the ligand as part of a larger binding surface on the convex face of the ECD. Alanine mutation of several residues on the convex face of ActRII-ECD has been shown to have no effect on activin- and inhibin-binding, and activin-dependent signaling of ActRII [13]. This further supports the existence of distinct ligand-binding sites on TβRII-ECD and ActRII-ECD (Fig. 5). However, it is possible that the disulfide bonds in finger 1 constrain a bioactive conformation of this surface loop, with a critical role played by the predicted anchor disulfide C54–C71. Further biochemical studies complemented by the experimental determination of the TβRII-ECD structure in the presence and absence of the ligand will be needed to clarify these issues.

Sequence analysis shows a high degree of conservation between the ECDs of various mammalian TβRIIs, and a somewhat lower sequence identity relative to the avian TβRII-ECD (Fig. 6). During the progress of this work, a TβRII from *Xenopus laevis* has been isolated and characterized [20]. Although this receptor displays only 67% amino acid similarity with human TβRII in the ECD portion, it binds TGF-β and supports a TGF-β-mediated response in HepG2 cells. A sequence alignment that includes not only the various mammalian and avian TβRII-ECD sequences, but also the sequence of the more distant yet functional *X. laevis* TβRII-ECD, would reveal the 'natural' mutagenesis of TβRII that occurred during evolution, and thus complement our site-directed mutational analysis data. As shown in Fig. 6, the seven residues of human TβRII, which belong to the hydrophobic patch on the concave face of the ECD, and which we found not to play a functional role, are also not identical in the sequences of the six TβRII species homologues. Residues V87, E98, V100, F133, and M135 in the human receptor correspond to isoleucine, serine, arginine, leucine, and threonine, respectively, in the *X. laevis* TβRII. Further comparison shows that human TβRII residues V85, V100, and F133 are replaced by alanine, isoleucine, and methionine, respectively, in the avian receptor, and that residue L97 aligns to an isoleucine in the porcine receptor. It is also interesting to note that residue H102 that was not mutated in this study, but which corresponds to the activin-binding site residue W60 of ActRII [13], is replaced by an aspartate in the porcine receptor, further supporting our finding of different ligand-binding sites on TβRII-ECD and ActRII-ECD. In contrast, the four cysteines in the finger 1 of the ECD are preserved in all six species homologues of TβRII. It appears that the sequence conservation is higher around the predicted disulfide C54–C71 than in the vicinity of the predicted disulfide C61–C67. This agrees with our finding that the C71A mutant receptor is functionally non-responsive to TGF-β whereas the C67A mutation retains the ligand-dependent signaling capability of the receptor. Finally, five acidic residues, D55, E78, E82, E142, and D145, of human TβRII are identical across the sequence alignment. Some of these residues may be engaged in specific electrostatic interactions (e.g. salt bridge or hydrogen bond) with the ligand, and more specifically with the critical TGF-β1 residue R94 [16]. A possible candidate for this interaction is D55, which is adjacent to the functionally important, predicted disulfide C54–C71.

Acknowledgements: The authors thank Lucie Bourget for her expert help with flow cytometry and Dr. Darrell Mousseau for assistance with the statistical analysis. This is NRCC publication No. 44805.

References

[1] Roberts, A.B. and Sporn, M.B. (1990) in: Handbook of Experimental Pharmacology, Peptide Growth Factors and Their Receptors (Sporn, M.B. and Roberts, A.B., Eds.), pp. 419–472, Springer, New York.
[2] Roberts, A.B. and Sporn, M.B. (1993) Growth Factors 8, 1–9.
[3] Wrana, H.L., Attisano, L., Carcamo, J., Zentella, A., Doody, J., Laiho, M., Wang, X.-F. and Massagué, J. (1992) Cell 71, 1003–1014.
[4] Laiho, M., Weis, F.M.B., Boyd, F.T., Igontz, R.A. and Massagué, J. (1991) J. Biol. Chem. 266, 9108–9112.
[5] Wrana, J.L., Attisano, L., Wieser, R., Ventura, F. and Massagué, J. (1994) Nature 370, 341–347.
[6] ten Dijke, P., Yamashita, H., Ichijo, H., Franzen, P., Laiho, M., Miyazono, K. and Heldin, C.H. (1994) Science 264, 101–104.
[7] Ventura, F., Doody, J., Liu, F., Wrana, J.L. and Massagué, J. (1994) EMBO J. 13, 5581–5589.
[8] Rodriguez, C., Chen, F., Weinberg, R.A. and Lodish, H.F. (1995) J. Biol. Chem. 270, 15919–15922.
[9] Wieser, R., Wrana, J.L. and Massagué, J. (1995) EMBO J. 14, 2199–2208.
[10] Souchelnysky, S., ten Dijke, P., Miyazono, K. and Heldin, C.-H. (1996) EMBO J. 15, 6231–6240.
[11] Pepin, M.-C., Beauchemin, M., Plamondon, J. and O'Connor-McCourt, M.D. (1996) Biochem. Biophys. Res. Commun. 220, 289–293.
[12] Guimond, A., Sulea, T., Pepin, M.-C. and O'Connor-McCourt, M.D. (1999) FEBS Lett. 456, 79–84.
[13] Gray, P.C., Greenwald, J., Blount, A.L., Kunitake, K.S., Donaldson, C.J., Choe, S. and Vale, W. (2000) J. Biol. Chem. 275, 3206–3212.
[14] Higuchi, Russell (1989) in: PCR Technology (Elrich, H.A., Ed.), pp. 61–70, Stockton Press, New York.
[15] Greenwald, J., Fischer, W.H., Vale, W.W. and Choe, S. (1999) Nat. Struct. Biol. 6, 18–22.
[16] Burmester, J.K., Qian, S.W., Ohlsen, D., Phan, S., Sporn, M.B. and Roberts, A.B. (1998) Growth Factors 15, 231–242.
[17] Wrana, J.L. and Attisano, L. (1996) Trends Genet. 12, 493–496.
[18] ten Dijke, P., Miyazono, K. and Heldin, C.H. (2000) Trends Biochem. Sci. 25, 64–70.
[19] Massagué, J. and Chen, Y.-G. (2000) Genes Dev. 14, 627–644.
[20] Dhanasekaran, S.M., Vempati, U.D. and Kondaiah, P. (2001) Gene 263, 171–178.